

Helium adsorbed on carbon nanotube bundles: one-dimensional and/or two-dimensional solids?

Tate Wilson and Oscar E. Vilches

Department of Physics, University of Washington, Seattle WA 98195-1560, USA
E-mail: vilches@phys.washington.edu

Heat capacity measurements of ^4He adsorbed on closed-end single-wall carbon nanotube bundles in the temperature range $1.5\text{ K} < T < 6\text{ K}$ are reported. Heats of adsorption Q_{st} calculated from isotherms measured on the same calorimeter cell are included. We correlate Q_{st} features with features of the helium heat capacity. We discuss possible interpretations of the current data.

PACS: **67.70.+n**, **68.43.-h**, **61.48.+c**

Single layer helium films physisorbed on exfoliated graphite have been studied in great detail, both experimentally and theoretically, for a long time [1–5]. These films provided, for the first time, realizations of several phases of matter in reduced dimensionality: two-dimensional (2D) gases and fluids [6–8], commensurate (CS) [9,10] and incommensurate (ICS) solids [11–13], as well as the phase transitions between them as a function of temperature and coverage.

A new carbon material discovered in the last decade is carbon nanotubes [14,15]. In the form of bundles or ropes, they have a rather large surface area per gram of material which makes them suitable for physisorption studies using somewhat conventional techniques. Although many types of carbon nanotubes exist, considerable theoretical [16–27] and some experimental [28–36] work has been done on the adsorption of many rare gas atoms and simple molecules deposited on closed-end single-wall carbon nanotube (SWNT) bundles. The attraction of the SWNT bundles is that on the interstitial channels between three nanotubes and on the grooves between two nanotubes on the outside surface of a bundle, one-dimensional (1D) chains of atoms/molecules can be adsorbed. These chains may be in the form of 1D gases and fluids if mobile [17,21,26,27] and perhaps commensurate and/or incommensurate solids [37]. Further adsorption on the outside surface of the bundles should lead to their coating with a monolayer that physically resembles adsorption on graphite, perhaps with different properties due to the curvature of the graphene surfaces, finite size, and confinement between grooves of the bundle [37]. A crossover from 1D to 2D or 3D proper-

ties is then possible, given that one can start with 1D chains that eventually, as a function of coverage and/or temperature, interact with each other in 2D and 3D space.

In this article we report on initial studies of the heat capacity of ^4He on SWNT bundles as a function of temperature and volume of gas adsorbed (coverage); these measurements are complemented by a few volumetric adsorption isotherms on the same bundles. Two previous somewhat indirect measurements of the heat capacity of ^4He on SWNT bundles have appeared [38,39]. In both cases, the prime intent of the measurement was to obtain the heat capacity of the nanotubes; ^4He was used as exchange gas to cool the bundles and/or the calorimeter and inner parts of the cryostat. The «nuisance» ^4He heat capacity had to be subtracted from the total. In Ref. 39 though, the ^4He excess heat capacity at an estimated 80% of monolayer completion was fitted by an expression of the form $C_{\text{film}} = \alpha T + \beta T^2$. In our measurements, performed over a wide range of ^4He coverages, we find heat capacities with the same temperature dependence, but with α and β being coverage dependent.

A theoretical study by Miller and Krostcheck [26] of ^4He using density functional theory predicts that at temperatures above $T = 0\text{ K}$ 1D ^4He is a gas/fluid, a result in agreement with expectations that in 1D there is no liquid-vapor critical point at finite temperature. At $T = 0\text{ K}$ these authors find coexistence between a very low density liquid (linear density, $\lambda = 0.036\text{ \AA}^{-1}$) and a zero density gas. Compression of this liquid leads to solidification at about $\lambda \approx 0.2\text{ \AA}^{-1}$. Studies of 1D ^4He by Gordillo et al. [21] and by Stan et al. [17]

deposited on the grooves of nanotube bundles support these results. These studies though use smoothed potentials with no atomic structure for the nanotubes. Including the atomic structure of the nanotubes may lead to the formation of novel commensurate structures [37]. A unique structure found for adsorption of heavier rare gases on SWNT bundles is a «three-line phase», predicted theoretically (see review by Calbi et al. [16]) and deduced from experiments by Talapatra and Migone [33] for Ar adsorption. This phase is formed after filling the outside grooves with 1D lines of atoms. The most favorable next place to add atoms is by forming three lines of atoms anchored at the grooves. Completion of the three-line phase should occur at a total coverage of about three times the amount of helium needed to form one compact line on the grooves.

Our experiments have searched for the 1D gas/fluid phase, the three-line phase, and the eventual crossover to 2D adsorption on a graphite-like surface (the exterior of the bundles between the grooves). In the following paragraphs we describe our experimental methods, the results obtained, and how the results relate to expectations.

The adsorption/heat capacity cell used in these measurements was made by pressing 100 mg of HiPcoTM nanotube bundles [40] between two very thin wall copper foils, soldering the edges, and adding a 1/16" diameter thin wall stainless steel capillary to serve as support, thermal link, and gas dosing line. The cell was connected to a room temperature gas dosing system. The cell was thermally connected via the fill line to a brass plate, which in turn was thermally connected to a pumped liquid ⁴He evaporator. The temperature of the intermediate plate could be regulated between 1.1 and 16 K; a brass shield thermally attached to the brass plate served to isolate the adsorption/heat capacity cell from the 4.2 K walls of the vacuum can. The cell had a thermometer and heater attached to opposite sides.

We started every set of measurements by pumping our adsorption cell at room temperature to the 10⁻⁷ Torr range. For adsorption isotherm measurements we kept the cell at the desired constant temperature; for each point we dosed helium in and waited for pressure equilibration, sometimes many hours. For the heat capacity measurements we dosed He at a temperature high enough that the equilibrium vapor pressure was in the 10⁻² Torr range for annealing purposes. We used the ac calorimetry method. After a frequency/amplitude scan of the T_{ac} oscillations, we chose to work at the highest possible frequency, which was 1 Hz. We were extremely careful to keep the pressure in the cell to less than 10 Torr while doing the

isotherms to prevent from blowing it into the vacuum can. For essentially all but one heat capacity measurement the pressure in the cell while doing the calorimetric measurements was always below 10⁻⁴ Torr, the smallest pressure we can measure, and no desorption heat capacity was observed.

While the adsorption isotherms on this cell show the same general features as the ones we obtained in an extensive study using other SWNT bundles made in Montpellier, France [41], the calculated isosteric heats, $Q_{st}/k_B = -\partial(\ln P)/\partial(1/T)$, at very low coverages appear to be substantially higher than on our earlier work, compare Figs. 1, *a* and 1, *b*. In particular, the extrapolated zero-coverage Q_{st}/k_B for this sample is about 400 K or more, Fig. 1, *a*, while for the Montpellier SWNT bundles we used in Ref. 36 the highest Q_{st} was approximately 240 K. This difference, in part, may come from different pumping times of the sample cells before the experiment (cleaning higher binding sites before experiments), but it may be entirely due to the different characteristics of the SWNT bundles [40,41]. We observe also that the fraction of gas adsorbed before reaching the graphite-like adsorption plateau is also larger (referred to coating the bun-

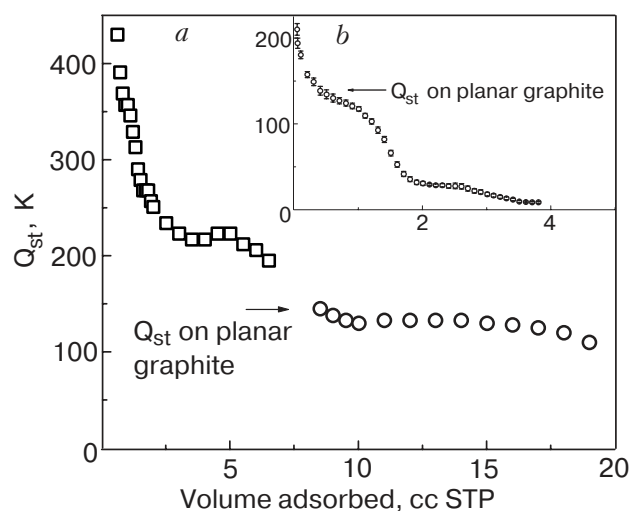


Fig. 1. (a) Isosteric heat of adsorption of ⁴He on HiPcoTM SWNT bundles [40], obtained from four isotherms on heat capacity cell at $T = 14$ and 16 K ($0 < V_{ads} < 7$ cc STP) and 9 and 11 K (8 cc STP $< V_{ads} < 11$ cc STP). (b) Isosteric heat of adsorption of ⁴He on Montpellier SWNT bundles [41], from extensive set of adsorption isotherms between 2.1 and 14 K, as reported in Ref. 36. Note the agreement in the isosteric heats between both SWNT samples at the graphite-like plateau, but the differences at low coverages both in Q_{st}/k_B and in the volume adsorbed compared to the one needed for completion of the plateau. Full monolayer coverage of the bundles though is not achieved until about 1.6 cc STP in *b* and about 24 cc STP (from heat capacity) in *a*.

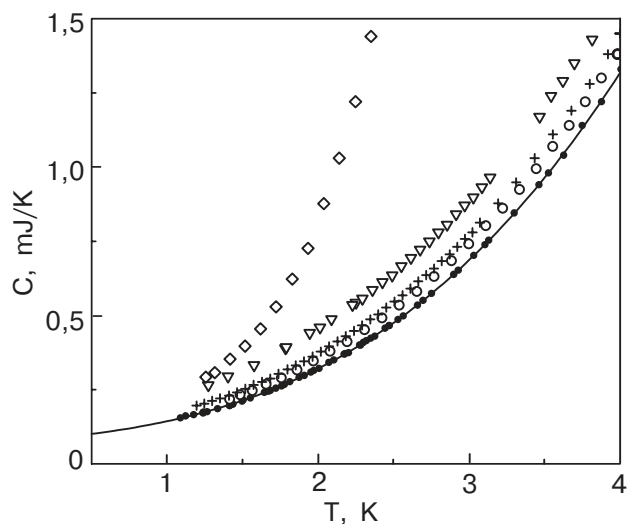


Fig. 2. Total measured heat capacity between 1.2 and 4 K: empty cell (\bullet), 3.2 cc STP (\circ), 6.3 cc STP ($+$), 15.8 cc STP (∇), 31.1 cc STP (\diamond). The solid line is the fit to the background used for obtaining the films heat capacity.

dles with a full monolayer) for this cell than for the one used in the previous work.

For the calorimetric measurements we measured first the empty cell heat capacity and assumed it to be constant. We then added (occasionally removed) controlled amounts of helium to (from) the cell and measured it again. The film heat capacity is the difference between each measurement and a polynomial fit to the background. Results for the total heat capacity for the empty cell (fitted solid line) and for the cell plus four films are shown in Fig. 2. The difference heat capacity for three of these films plus three other films is shown in Fig. 3,*a*. Although we have measured several more coverages than shown, the ones of Fig. 3,*a* are representative of the different regions of the Q_{st}/k_B vs. amount of gas adsorbed graph, Fig. 1,*a*. The film at 31.1 cc STP shown in Fig. 2 clearly demonstrates desorption in its exponential temperature dependence, confirmed by the measurable increasing vapor pressure. It is not included in the discussion.

We begin our discussion of the results by emphasizing that none of the measured specific heats is constant with temperature, not even at the lowest coverage we have measured (about 0.75 cc STP). The scatter in the film heat capacity at lower coverages is very high; improvements will require a modification of our experimental setup. Thus we do not find a 1D (at the lowest coverage) or 2D (when graphite-like adsorption starts), almost ideal gas regime as observed for both helium isotopes on graphite (2D) over the lower density half of the first adsorbed layer. On the contrary, the heat capacities measured all increase

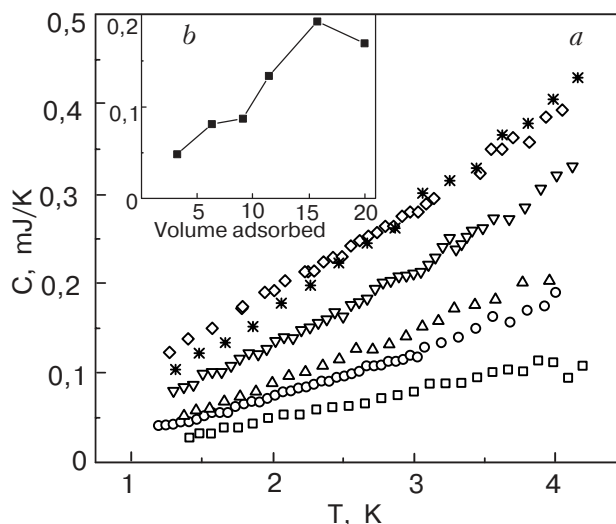


Fig. 3. (a) Heat capacity of ^4He adsorbed/SWNT bundles: 3.2 cc STP (\square), 6.3 cc STP (\circ), 9.1 cc STP (\triangle), 11.5 cc STP (∇), 15.8 cc STP (\diamond), 20.1 cc STP ($*$). (b) The total heat capacity vs. volume adsorbed at 2 K. Note the two well separated regimes, below and above 9 to 10 cc STP, corresponding to features in Q_{st}/k_B in Fig. 1,*a*.

steadily with temperature, albeit with some significant variations in their temperature dependence. Furthermore, all measured heat capacities appear to be too small for what one would expect for 1D or 2D solids with Debye temperatures comparable to those for ^4He in 2D or 3D for similar interatomic spacings. This may be due to a portion of the SWNT bundles not being in good thermal contact with the outside wall of the calorimeter cell, although it could be due too to some intrinsic property of these new type of helium films.

The very high binding energy at very low coverage ($Q_{st}/k_B \approx 450$ K at $V_{ads} \approx 0$) likely leads to very localized atoms and possibly very small specific heats. With moderate increases in coverage the heat capacity increases rapidly, correlated with the rapid decrease in Q_{st}/k_B . Figure 3,*b* shows a heat capacity isotherm at 2 K for this set of data. By about 3 cc STP adsorbed the growth in heat capacity slows down. This slowing down corresponds to the slight rise in Q_{st} in Fig. 1,*a*. By about 9 to 10 cc STP adsorbed the heat capacity suddenly starts to rise again. This feature corresponds very well with starting adsorption on a surface with Q_{st} comparable to the one of ^4He on graphite, Fig. 1,*a*. Increases in heat capacity with coverage stop at 16 to 17 cc STP adsorbed; from then on the total heat capacity decreases with increasing coverage, much like it does for both helium isotopes on graphite when 2D incommensurate solids (ICS) form. On graphite, these 2D ICS exist at densities above 0.079 \AA^{-2} . Nevertheless, a direct comparison with He/graphite,

as assumed in Ref. 39, can not be made. For the lowest 2D solid density melting occurs at $T = 1$ K; the melting temperature increases rather uniformly with increasing coverage. At temperatures above melting the specific heat becomes constant and near $0.9k_B$ per atom, a signal of a compressed 2D almost classical gas/fluid. For our system of He/SWNT bundles there is no observation of melting and no observation of a constant specific heat.

One possible scenario for different film/SWNT bundles regimes is the following. First, adsorption occurs in the outside grooves of the bundles in the form of very localized linear chains of helium atoms. Heterogeneous and uniform sites are occupied, and at about 3 cc STP all possible linear chains have been formed. This regime is now followed by adsorption on lines parallel and next to the atoms in the linear (groove) phase, similar to the case for Ar/SWNT bundles [16,33]. The maximum capacity of this phase is reached then, for our cell, at 9 to 10 cc STP. The increase we observe in Q_{st} at ≈ 4 cc STP could be associated with the latent heat of condensation of this phase. On a third adsorption stage, the space between the three-lines begins to be filled. This is adsorption on a bare, graphite-like curved surface, but in narrow strips between the anchored three lines of atoms. These strips could be rather long compared to their width. Simple geometric estimates using the density of helium on graphite give that up to 4 or 5 compressed lines of ^4He could be formed at full density in spaces between adjacent grooves on the «flat» facets of bundles, and that 7 to 9 compressed lines could be formed on «corner tubes» between facets of the bundles. It is remarkable that for 37 nanotubes ideal bundles (they have 18 outside grooves) the total additive coverages measured in lines of atoms, for the 1D groove phase, three-line phase, and graphite like adsorption will be in the ratio 18:54:138 at completion of the solid monolayer on a SWNT bundle, or 39% of adsorbed atoms would be in the three lines per groove phase. Looking at Fig. 1,a and the heat capacity measurements, completion of a first layer of atoms in our cell occurs at about 24 cc STP. If completion of the three-line phase is at 10 cc STP, experimentally we have 42% of a monolayer atoms in that phase, remarkably close to the geometric estimate with no adsorption on interstitial channels.

In conclusion, we have measured adsorption isotherms and the heat capacity of ^4He adsorbed on SWNT bundles using the same cell for both measurements. We have been able to correlate features of the isosteric heat with those of the heat capacity. We have not found a 1D or 2D gas phase formed by the adsorbed atoms, rather we observe a temperature de-

pendence of the heat capacity that can be fitted to an expression of the form $C \approx \alpha T + \beta T^2$, with both coefficients being coverage dependent. We are continuing our experiments to obtain a complete description of the evolution of this 1D/2D system.

This research was supported by the USA NSF, grant 986767 and 0115663. We acknowledge very useful discussions with M.W. Cole, M. Kostov, R.B. Hallock, K. Johnson, A.D. Migone, J.G. Dash, D. Cobden, J. Rehr, and M. den Nijs. Discussions with K. Chishko, L. Firllej, and B. Kuchta at the CC'2002 conference, and receiving some of their data prior to publication have been extremely valuable.

1. J.G. Dash, *Films on Solid Surfaces*, Academic Press, New York (1975).
2. H. Godfrin and H.J. Lauter, in: *Progress in Low Temperature Physics*, Vol. XIV, W.P. Halperin (ed.), North-Holland, Amsterdam (1995), p. 213.
3. L.W. Bruch, M.W. Cole, and E. Zaremba, *Physical Adsorption: Forces and Phenomena*, Clarendon Press, Oxford (1997).
4. M.E. Pierce and E. Manousakis, *Phys. Rev.* **B62**, 5228 (2000).
5. T.N. Antsygina, I.I. Poltavsky, M.I. Poltavskaya, and K.A. Chishko, *Fiz. Nizk. Temp.* **28**, 621 (2002) [*Low Temp. Phys.* **28**, 442 (2002)].
6. M. Bretz, J.G. Dash, D.C. Hickernell, E.O. McLean, and O.E. Vilches, *Phys. Rev.* **A8**, 1589 (1973); *ibid.* **A9**, 2814 (1974).
7. R.E. Ecke, Q.S. Shu, T.S. Sullivan, and O.E. Vilches, *Phys. Rev.* **B31**, 448 (1985).
8. D.S. Greywall and P.A. Busch, *Phys. Rev. Lett.* **67**, 3535 (1991).
9. M. Bretz, *Phys. Rev. Lett.* **38**, 501 (1997).
10. M.J. Tejwani, O. Ferreira, and O.E. Vilches, *Phys. Rev. Lett.* **44**, 152 (1980).
11. R.L. Elgin and D.L. Goodstein, *Phys. Rev.* **A9**, 2657 (1974).
12. S.V. Hering, S.W. Van Sciver, and O.E. Vilches, *J. Low Temp. Phys.* **25**, 789 (1976).
13. D.S. Greywall, *Phys. Rev.* **B47**, 309 (1993).
14. S. Iijima, *Nature (London)* **354**, 56 (1991); S. Iijima and T. Ichihashi, *ibid.* **363**, 603 (1993).
15. B.Y. Jacobson and R.E. Smalley, *Scientific American* **85**, 324 (1997).
16. M.M. Calbi, M.W. Cole, S.M. Gatica, M.J. Bojan, and G. Stan, *Rev. Mod. Phys.* **73**, 857 (2001).
17. G. Stan, V.H. Crespi, M.W. Cole, and M. Boninsegni, *J. Low Temp. Phys.* **113**, 447 (1998).
18. Q. Wang, S.R. Challa, S.S. Scholl, and J.K. Johnson, *Phys. Rev. Lett.* **82**, 956 (1999).
19. S.M. Gatica, M.W. Cole, G. Stan, J.M. Hartman, and V.H. Crespi, *Phys. Rev.* **B62**, 9989 (2000).
20. K.A. Williams and P.C. Eklund, *Chem. Phys. Lett.* **320**, 352 (2000).

21. M.C. Gordillo, J. Boronat, and J. Casulleras, *Phys. Rev. Lett.* **85**, 2348 (2000); *Phys. Rev.* **B61**, R878 (2000); *Phys. Rev.* **B65**, 014503 (2002).
22. M.W. Cole, V.H. Crespi, G. Stan, C. Ebner, J.M. Hartman, S. Moroni, and M. Boninsegni, *Phys. Rev. Lett.* **84**, 3883 (2000).
23. M. Boninsegni, S-Y. Lee, and V.H. Crespi, *Phys. Rev. Lett.* **86**, 3360 (2001).
24. M.K. Kostov et al., *J. Chem. Phys.* **116**, 1720 (2002).
25. M.M. Calbi and M.W. Cole, *Phys. Rev.* **B66**, 115413 (2002).
26. E. Krotscheck and M.D. Miller, *Phys. Rev.* **B60**, 13038 (1999).
27. A. Siber, *Phys. Rev.* **B66**, 205406 (2002).
28. W. Teizer, R.B. Hallock, E. Dujardin, and T.W. Ebbesen, *Phys. Rev. Lett.* **82**, 5305 (1999); *ibid.* **84**, 1844(E) (2000).
29. S. Talapatra, A.Z. Zambano, S.E. Weber, and A.D. Migone, *Phys. Rev. Lett.* **85**, 138 (2000).
30. S.E. Weber, S. Talapatra, C. Journet, A. Zambano, and A.D. Migone, *Phys. Rev.* **B61**, 13150 (2000).
31. M. Muris et al., *Langmuir* **16**, 7019 (2000).
32. M. Muris, N. Dupont-Pavlovsky, M. Bienfait, and P. Zeppenfeld, *Surf. Sci.* **492**, 67 (2000).
33. S. Talapatra and A.D. Migone, *Phys. Rev. Lett.* **87**, 206106 (2001).
34. Y.H. Kahng, R.B. Hallock, E. Dujardin, and T.W. Ebbesen, *J. Low Temp. Phys.* **126**, 223 (2002).
35. T. Wilson, A. Tyburski, M.R. DePies, O.E. Vilches, D. Becquet, and M. Bienfait, *J. Low Temp. Phys.* **126**, 403 (2002).
36. T. Wilson and O.E. Vilches, accepted for publication in *Physica B* (April 2003).
37. L. Firlej and B. Kuchta have modeled numerically the adsorption of He on a single carbon nanotube and a bundle of three nanotubes, observing the formation of a commensurate phase (private communication).
38. J. Hone, B. Battlogg, Z. Benes, A.T. Johnson, and J.E. Fischer, *Science* **289**, 1730 (2002).
39. J.C. Lasjounias, K. Biljakovic, Z. Benes, J.E. Fischer, and P. Monceau, *Phys. Rev.* **B65**, 113409 (2002).
40. HiPco™ SWNT bundles, prepared by laser ablation using Fe as catalyst, can be purchased from Carbon Nanotechnologies. Our particular sample had 98% bundles. The diameter of the individual nanotubes is stated as about 1 nm.
41. We thank Prof. Michel Bienfait from CRMC2 and Luminy, Marseille, France, for giving us a sample of SWNT bundles fabricated in Montpellier, France, see C. Journet et al., *Nature (London)* **388**, 756 (1997). These bundles were made by the electric-arc method using Ni-Y as catalyst and are not purified. The diameter of these nanotubes is about 1.3 nm, with 1.7 nm between adjacent nanotubes in the bundles.